Author/s:
Raja, BNK;Miramini, S;Duffield, C;Chen, S;Zhang, L

Title:
A Simplified Methodology for Condition Assessment of Bridge Bearings Using Vibration Based Structural Health Monitoring Techniques

Date:
2021-09-01

Citation:
Raja, B. N. K., Miramini, S., Duffield, C., Chen, S. & Zhang, L. (2021). A Simplified Methodology for Condition Assessment of Bridge Bearings Using Vibration Based Structural Health Monitoring Techniques. INTERNATIONAL JOURNAL OF STRUCTURAL STABILITY AND DYNAMICS, 21 (10), https://doi.org/10.1142/S0219455421501339.

Persistent Link:
https://hdl.handle.net/11343/292046

A simplified methodology for condition assessment of bridge bearings using vibration based structural health monitoring techniques.

Babar Nasim Khan Raja, Saeed Miramini, Colin Duffield, Shilun Chen, Lihai Zhang*
Department of Infrastructure Engineering, University of Melbourne, Victoria 3010, Australia
Correspondence:
Lihai Zhang
Department of Infrastructure Engineering, University of Melbourne, Victoria 3010, Australia
Email: lihzhang@unimelb.edu.au

Abstract

The mechanical properties of bridge bearings gradually deteriorate over time resulting from daily traffic loading and harsh environmental conditions. However, structural health monitoring of in-service bridge bearings is rather challenging. This study presents a bridge bearing condition assessment framework which integrates the vibration data from a non-contact interferometric radar (*i.e.*, IBIS-S) and a simplified analytical model. Using two existing concrete bridges in Australia as a case study, it demonstrates that the developed framework has the capability of detecting the structural condition of the bridge bearings in real-time. In addition, the results from a series of parametric studies show that effectiveness of the developed framework is largely determined by the stiffness ratio between bridge bearing and girder (*R*), *i.e.* the structural condition of the bearings can only be effectively captured when the value of *R* ranges from 1/100 and 100.

Keywords: bridge bearing; interferometric radar (IBIS-S); structural health monitoring; bridge natural frequency

1 Introduction

Bridges are progressively deteriorating due to heavy loadings and environmental conditions (e.g. corrosion and erosion)[1-9]. The continuous degradation of the structural components of the bridge could ultimately lead to expensive retrofitting or even bridge collapse.[9-12] Therefore, damage detection and application of necessary retrofitting techniques at an early stage become necessary for prolonging the service life of the bridges.[13-15]

Bridge bearings are one of the important components of a bridge that provides a resting interface between the bridge deck and pier. The purpose of bearings is to transfer the loading from the bridge superstructure to substructure and also to allow the horizontal movement of the superstructure due to expansion and contraction, and rotation caused by self-weight and other external loads.[16, 17] Besides, elastomeric bearings are extensively used for seismic isolation of the superstructure, and deterioration in bearing mechanical properties may significantly affect the seismic response of both the superstructure and substructure.[18] The most commonly used bridge bearings are steel reinforced elastomeric-bearing pads (SERBs), which can deform substantially over time without damage. They are usually flexible under uniaxial stress and shear and very stiff against any volume change.[17] As it is challenging for the service life of a bridge bearing to meet the bridge design requirements, regular structural health monitoring of the bridge bearing becomes necessary.[19] The study of Reoder et al. (1987)[20] on the performance of elastomeric bearings revealed that the stiffness of rubber can increase as high as 50 times under low-temperature conditions, while continuous fatigue loading could induce widespread cracks and tearing

in the elastomers. Also, Stanton et al. (1982)[21] have suggested that in some cases the excessive deformation in bearing pads can lead to the service limit state failure of the bridge. Furthermore, Dicleli and Bruneau (1995)[22] identified bearing pads as the weakest link of a structural system during seismic excitation, and a minor earthquake can cause severe damage to the bearings of a bridge.[23]

Akbari et al. (1994)[16] conducted a series of field testing of more than 1000 bridge bearings. They found that around 85% of the inspected bridges had defective bearings with an average of 18 different types of bearing defects per bridge. The major types of damage observed in bridge bearings included splitting of steel and elastomeric layers, tearing and crushing of elastomer, aging, and weathering, deviation from specified mechanical properties, slip out and bulging as well as disintegration. However, the actual extent of damage to bridge bearings was difficult to quantify.

Currently, one of the commonly used bearing inspection methods is visual inspection, which is subjective, time-consuming, and unable to provide a quantitative evaluation of the bearing conditions.[16, 19] Also, as the mechanical testing for bearing condition assessment requires the collection of bearing samples from the bridges, it becomes costly and impractical. The vibration-based damage detection technique is one of the many commonly used methods for damage detection by monitoring the change in the dynamic characteristics of the bridges.[14, 24-27] A bridge structure is a dynamic system with its dynamic characteristics affected by mass, stiffness, and damping.[28-32] Thus, the deterioration of bridge bearings could affect support stiffness of the bridge, and ultimately the overall dynamic characteristics of the bridge (e.g. natural frequencies).[33]

Studies have been carried out to determine a relationship between the dynamic characteristic of a system and the condition of bridge bearings supports.[27, 34-39] Fayyadh et al. (2012)[40] considered the dynamic properties of a beam as a way of monitoring the support condition and concluded that the bending mode shapes and natural frequency of a system can be used to assess the extent of damage or deterioration in elastic bearing supports. In addition, Macbain and Genin (1973)[41] studied the effect of support stiffness on the fundamental frequency of fixed end beam and a cantilever beam, they concluded that, in comparison to shear deformation and rotary inertia, the effect of support condition on fundamental frequency is more obvious. They also developed the expressions for fundamental frequency as a function of support stiffness and length to depth ratio. Similarly, Rao and Mirza (1989)[42] found that both translation and rotational stiffness of beam supports have a significant effect on the first three mode shapes and respective frequencies of a beam, the higher frequencies and mode shapes are less sensitive to the support stiffness. Carne et al.[43] studied the effect of support stiffness on measured modal frequencies and developed the single degree of freedom (SDOF) and multiple degrees of freedom model systems. They proposed

a relationship between the increase in measured frequencies and square of the ratio of frequencies of rigid body mode and elastic modes.

The fundamental frequency has also an important role to control the excessive vibrations in bridges under moving loads. For example, to avoid resonance the fundamental frequency of the bridge is usually adjusted away from 1.5 Hz to 4.5Hz, which is the common natural frequency range for trucks.[44, 45] For a simply supported girder bridge, the recommended lower limit for natural frequency is 3.0 Hz in China, 3.32 Hz in Russia, and 3.5 Hz in America.[46] Based on the bridge design specifications of Ontario (Ontario Highway Bridge Design Code, OHBDC) and Australia, the relationship between fundamental frequency and live load deflection is used for vibration control in bridges.[47] The dynamic impact factor in most bridge design specifications is also based on the natural frequency of a bridge.[48] OHBDC recommends an increase in the dynamic amplification factor if the dominant frequency of a structure is in the range of 2–5 Hz.[49] Also, Barots (1995)[50] proposed an increase in the dynamic amplification factor for structures with a fundamental frequency between 1.5 Hz and 5 Hz. Therefore, the change in bearing stiffness can lead to the change in overall vibration response of the bridge structure.

To date, effective and efficient methods for structural health monitoring of bridge bearings are lacking and research work in this field is limited. In addition, the dynamic analysis of bridges using finite element (FE) analysis is very time-consuming in the preparation of data based on "as-built" bridge construction drawings and program execution. Therefore, the purpose of this study is to develop an innovative methodology involving a SDOF model and the interferometric radar (IBIS-FS) for assessing deterioration of the mechanical stiffness of the bridge bearings. The model was validated through finite element modelling and the inspection data of two bridges in Melbourne, Australia, through field testing using IBIS-FS. A series of parametric studies were then carried out to explore the limitation of the developed model and the effect of variation in elastic support stiffnesses on the dynamic characteristics of the overall system.

2 Problem statement

Two Australian bridges are taken as a case study for the developed analytical model implementation: (1) Merlynston Creek Bridge, (M-80, Melbourne, Australia) and (2) Port of Melbourne Bridge (PoM, Appleton Dock Road, Port Melbourne, Australia). Constructed in 1996, the M-80 Bridge is a three-span prestressed concrete girder bridge, which was extensively studied in our previous studies.[27] The previously collected data of the M-80 Bridge was used to validate the model predictions. The Port of Melbourne Bridge (PoM), a multiple span bridge with varying span length, was constructed in 2009 using super T-girders and a 180 mm thick concrete bridge deck. A typical span of PoM Bridge (30.5 m length x 30 m width) with 13 super T-girders (1500 mm in depth) supported

by elastomeric-bearing pads on bridge piers was considered in this study. The FE models of the selected bridges were developed and validated through field investigation data of the respective bridges. The effect of support stiffness variation on the fundamental frequency of bridge was further evaluated using validated FE models. Finally, a generalised SDOF model was developed and calibrated through the FE models along with field test results. The model establishes the relationship between fundamental frequency and support stiffness of the bridge.

3 Methods

As shown in Figure 1, a schematic diagram for the proposed methodology is presented for monitoring the mechanical properties of the bridge bearings using the SDOF model in conjunction with bridge testing using IBIS-FS. IBIS-FS has the capability of remotely detecting the changes in natural frequencies of the bridges under operational conditions conveniently and efficiently with high accuracy.[27] In the first step, the FE models of two prestressed girder bridges supported on elastomeric bearings, situated in Melbourne, Australia, were developed and validated through the field-testing using IBIS-FS. An analytical simplified single degree of freedom (SDOF) model was developed and calibrated using the validated finite element model. The "as-built" material and geometric properties of a bridge, as well as mechanical properties of bridge bearing pads, were input into the proposed SDOF model to predict the natural frequency (f_1) of an intact bridge. The predicted results are then compared with the current natural frequency (f_1') of the bridge obtained using IBIS-FS measurements. The difference between the measured frequency and calculated using the SDOF model would estimate the change in the mechanical properties of the bearings. For practising engineers, the FE calibration as shown in Figure 1 is not required, only simplified model and field-testing using IBIS-FS would give the estimate of in-service bearing stiffness.

3.1 *FE modelling of concrete bridges*

The purpose of the FE modelling is to explore the effect of support stiffnesses on the fundamental frequency of the bridge. First, the three-dimensional (3D) FE models of the bridges were constructed and validated using IBIS-FS results. Then, a series of parametric studies were carried out by varying the support conditions, and the respective variation in the fundamental frequency is studied. Finally, the FE model results were used to calibrate the developed analytical model and study the limitations of SDOF system under different conditions.

As shown in Figure 2, the 3D FE models of the bridges were constructed based on the "as-built" construction drawings of the bridge. While the concrete girders and slabs were modelled using 3D solid elements, truss elements were used to model steel bars and prestressing tendons. In the current FE analysis, the displacement

compatibility between rebar and concrete elements was ensured. Also, the elastomeric-bearing pads were modelled as an elastic spring with stiffness equal to the bearing pads. The material properties are shown in Table 1.

The two bridges were numerically analysed using eigenfrequency analysis of commercial FE package COMSOL MULTIPHYSICS v. 5.4.[51] A mesh convergence analysis was conducted to determine the optimum mesh size for the model, and the numerical model was solved using the eigenfrequency solver with relative tolerances of 1.0E-6 for the fundamental natural frequency of the bridges. The mesh sizes were chosen such that the differences between subsequent solutions in the convergence analysis were less than 1%. The entire geometry has meshed with built-in fine (0.35–2.44 m) tetrahedral elements.

3.2 *Measuring the dynamic characteristics of a bridge using IBIS-FS radar*

Figure 3 shows the field-testing setup for Port Melbourne (PoM) bridge. A non-contact remote IBIS-FS system is used in this work which consists of a portable power unit, a sensor module, and a control PC. IBIS-FS is a radar-based system that measures the object displacement by comparing the phase differences of the electromagnetic (EM) signals reflected from measurement points at different times.[27] It is based on the Stepped-Frequency Continuous Wave (CW-SF) technique along with microwave interferometry to detect multiple target points along the radar line of sight. The minimum distance required between two target points to be detected individually is defined as the range resolution, the respective area is called the range bin. The IBIS sensors obtain high range resolution with an electromagnetic sweep of large frequency bandwidth which can be defined as,

$$\Delta r = \frac{c}{2B} \tag{1}$$

where Δr is range bin[27], c is the speed of light and B is the frequency bandwidth. Higher bandwidth will result in a higher range resolution (shorter range bin). The large bandwidth is achieved by transmitting a burst of N single pulses of discrete electromagnetic waves with a constant increment in frequency Δf. That is,

$$B = (N-1)\Delta f \tag{2}$$

The response is measured in the frequency domain for N discrete frequencies with data consisting of vectors of N complex samples representing the radar echo (signals) from the respective range bin. The amplitude of the echo is the reflectivity of the target. The measured response is then reconstructed in the equivalent time domain using Inverse Discrete Fourier Transformation. The interferometric technique provides the line of sight displacement of all the reflectors by measuring the difference in the phase angle of EM waves reflected from the object at different times.[27] That is,

$$d_r = \frac{\lambda}{4\pi}\Delta\theta \quad (3)$$

where λ is the wavelength of EM signals and $\Delta\theta$ is phase shift.

3.3 *Development of SDOF model*

The governing equation of motion of a bridge girder supported by elastic bearings in the transverse direction can be described as,

$$EI\frac{\partial^4 y}{\partial x^4}(x,t) + \rho A\frac{\partial^2 y}{\partial t^2}(x,t) = 0 \quad (4)$$

where *y* is the transverse displacement; *x* is the distance along the length of the girder; *A*, ρ and *EI* are the cross-sectional area, mass density, and flexural rigidity of the bridge girder, respectively. The boundary conditions for the beam resting on elastic supports are as follows:

at *x=0*,

$$EI\frac{\partial^3 y\ (0,t)}{\partial x^3} = -k_{s1}y(0,t), \qquad EI\frac{\partial^2 y\ (0,t)}{\partial x^2} = 0 \quad (5a, b)$$

at *x=l*,

$$EI\frac{\partial^3 y\ (l,t)}{\partial x^3} = k_{s2}y(l,t), \qquad EI\frac{\partial^2 y\ (0,t)}{\partial x^2} = 0 \quad (6a, b)$$

Using the method of separation of variable, the free vibration solution can be expressed as,

$$y(x,t) = \sum_{n=1}^{\infty} Y_n(x)T(t) \quad (7)$$

where y_n (x) is the *n*-th mode of natural vibration, which is given by,

$$Y_n(x) = C_1\cosh\beta x + C_2\sinh\beta x + C_3\cos\beta x + C_4\sin\beta x \quad (8)$$

$$\beta^4 = (\alpha/L)^4 = {\omega_n}^2\rho A/EI \quad (9)$$

$$\omega_n = \alpha^2\sqrt{\frac{EI}{\rho AL^3}} \quad (10)$$

where ω_n is natural frequency of the girder beam, and α is the mode-dependent coefficient. Eq. (7) and (8) along with initial boundary conditions result in four homogeneous equations with four constants (i.e. C_1, C_2, C_3, and C_4). Solving the governing equations simultaneously yields the complex frequency equations for girder beams with elastic restraints. The complex partial differentiation-based models on the vibration-based characteristic of an elastic support system can be obtained by using the study of Kang and Kim (1996).[36]

To expedite the complex dynamic analysis, there are well known techniques available in the textbooks for simplifying a structure with distributed masses into an equivalent generalized lumped mass single-degree-of-freedom (SDOF)[52]. A simplified SDOF system was implemented in this study (Figure 4) considering both the

bridge girder and bridge bearing stiffnesses. The bridge girder is taken as an individual member with mass and stiffness, vertically supported on elastic springs. The equation of motion for free-response of given SDOF system is given as;

$$m_0.\frac{d^2y}{dx^2}\,(t) + K_e.y(t) = 0 \tag{11}$$

Considering the simple harmonic oscillations and solving Eq. (11) results the fundamental frequency of the system as

$$f_1 = \frac{1}{2\pi}\sqrt{\frac{K_e}{m_0}} \tag{12}$$

where m_o is the lumped mass of the bridge girder; and K_e is the effective stiffness of the bridge which is dependent on the elastic stiffness of beam with rigid vertical supports (k_b) (Table 2) and the support stiffness (k_s). That is,

$$K_e = \frac{(k_{s1} + k_{s2})\times k_b}{k_b + k_{s1} + k_{s2}} \tag{13}$$

where k_{s1} and k_{s2} are the stiffnesses of two bearing supports. Assuming the same stiffness of bearing pads on both ends of the bridge girder, Eq. (13) can be simplified as,

$$K_e = \frac{2k_s \times k_b}{k_b + 2k_s} \tag{14}$$

3.3.1 Semi-continuous / partially restrained supports

The support rotational restraints also have an impact on the overall stiffness of flexural members, ultimately the bending moment distribution, deflections, and natural frequencies of the member. Several simplified models have been developed for conventional continuous or discontinuous structural systems (moment distribution method, slope deflection method, stiffness matrix method, etc.). As shown in Figure 5a, the superstructure of a bridge usually consists of precast girders resting on simple supports and a continuous deck slab which may partially restrain the rotation at the ends of bridge girders resulting so-called "semi-rigid" end restraints.[53] Several simplified models have been developed to describe the semi-rigid support conditions using power, polynomial, and exponential functions.[54] In this study, the beam stiffness under different end restraint condition is given as,

$$k_b = \alpha^4 \times EI/L^3 \tag{15}$$

here α is a parameter describing the end restraints of a bridge girder (refer to Table 2). In Table 2 the continuous/fully restrained column refer to the end conditions where both the girders and the deck slab are continuous. Whereas the semi-continuous/partially restrained refer to the end conditions when the bridge girder is simply supported but the deck slab is continuous as depicted in Figure 5a. For the semi rigid restraints, the factor κ is introduced in this study which is defined as the stiffness coefficient of the bridge which incorporates

the effects of semi-rigid restraints conditions to the elastic stiffness of the bridge girder. The value of κ depends on the ratio between the flexural rigidity of continuous section of the bridge *(EI)* (i.e., slab) and the bending stiffness of the overall section, $n = (E_cI_c) / (E_bI_b/L_b)$ where E_b, I_b, and L_b are Young's modulus, the moment of inertia and span of a bridge girder; E_c and I_c are Young's modulus and moment of inertia of bridge deck. It can be obtained from the developed design chart (Figure 5b) generated by using FE analysis. Using a simple bridge girder as an example, Figure 5b shows that the value of κ generally increases with the increase of the ratio of flexural rigidity of continuous slab deck and bending stiffness of the girder beam $n = (E_cI_c) / (E_bI_b/L_b)$. In addition, it can be seen from Figure 5b that the length of the bridge girder has limited influence in the value of κ. The results are consistent with the study of Duarte da Costa et al. (2017)[55] and Couchman (1997).[56]

4 Results and Discussion

4.1 *Measuring natural frequencies of the bridges using IBIS-FS*

As shown in Figure 3, the dynamic characteristics of the PoM Bridge under traffic loading were monitored using IBIS-FS. Figure 3c shows the intensity of the radar signal echoes reflected from different points on the bridge as a function of the structure range profile. The obtained displacement response spectra from the test point in the frequency domain are shown in Figure 3d, which leads to a fundamental frequency of 4.1Hz. Similarly, the data obtained from our previous fieldwork using IBIS-FS for the M-80 Bridge shows that the fundamental frequency for the bridge was 9.4 Hz.[27]

4.2 *The finite element model validations*

Table 3 shows the comparison between the finite element model and field-testing results. It shows that the finite element model predictions are remarkably well in accordance with the field testing results.

4.3 *Prediction of natural frequencies of the bridges using the SDOF model*

The SDOF model developed in *Section 3.3* was validated using field testing results of IBIS-FS. The mechanical and material properties of the M-80 and PoM bridges used in the Eq. (12)– (15) are shown in Tables 1 and Table 4. The boundary conditions of the bridge girders were determined based on bridge stiffness coefficient (κ) depending on the ratio of flexural rigidity of continuous slab deck and bending stiffness of the girder beam $n = (E_cI_c) / (E_bI_b/L_b)$. The stiffness of the bearing pads used in this model was based on the "as-built" construction information of the bridges.

Table 5 shows the comparison of SDOF to IBIS-FS test results. It demonstrates that SDOF can predict the fundamental natural frequency of M-80 and PoM bridges reasonably well. This indicates that the developed SDOF can capture the dynamic behaviour of a bridge.

4.4 *Parametric studies*

4.4.1 SDOF model calibration with the FE model

As shown in the previous section, both the FE model and the SDOF model were able to predict the dynamic characteristic of the selected bridges. The validated FE model was further utilised to calibrate the SDOF model for different support stiffnesses of the bridge. The support stiffnesses were varied from *0.1 kN/mm to 100,000 kN/mm* using the FE model and the corresponding change in fundamental frequencies of the bridges are plotted in Figure 6. The same support stiffness parameters were tested on the developed SDOF model to predict the respective fundamental frequency of the structure. The analytical model results are also plotted in the same figure along with FE model predictions. It can be seen that SDOF model predictions are matching remarkably well with the FE model predictions for any support stiffness.

4.4.2 Effect of bearing stiffness on the fundamental frequency of bridges

This section investigates the effect of bearing stiffness on the fundamental frequency of the M-80 and PoM bridges. Figure 6 showed that the developed SDOF model can predict the change in the fundamental frequencies of these two bridges due to the change of bearing stiffness, and the prediction results are consistent with FE analysis results. The fundamental frequency of a bridge (f_1) initially increases with the increase of bearing stiffness (k_s) from *0.1 to 1000 kN/mm*, and then gradually reaches to a steady-state. This indicates that the change in bearing stiffness has an impact on the overall frequency of the bridge within a certain range, therefore the use of developed SDOF is limited. In the current study, the monitoring of fundamental natural frequencies of the M-80 and PoM bridges is only effective when the value of k_s is relatively low (i.e. <1000 KN/mm).

4.4.3 *Effect of support to girder stiffness ratio ($\boldsymbol{k_s/k_b}$)*

As shown in Eq. (12)– (15), the dynamic behaviour of a bridge is significantly influenced by the stiffnesses of the bridge girders (i.e. k_b) and their support conditions (i.e. k_s). Figure 7 shows the effect of support to girder stiffness ratio *(R)* on the fundamental frequency of the system for the two selected bridges. The change in the fundamental frequency of system with respect to the girder stiffness is plotted against the stiffness ratios. It is observed that the

change in frequency ratio always follows the same trend regardless of the support condition. For higher stiffness ratio the system behaves as a beam supported on rigid supports and the governing frequency is the frequency of the girder. Whereas for low stiffness ratios, the girder acts as a rigid mass and the stiffness of the supports determines the fundamental frequency of the overall system.

Figure 8 presents the percent change in natural frequency with the change in the ratio between the supports (k_s) to girder beam stiffness (k_b) (i.e. $R = k_s/k_b$). It shows that the variation in fundamental frequency is noticeable only within a certain range (i.e. R = 1/100 to 100). Therefore, the developed SDOF model can effectively predict the change in fundamental natural frequency when R falls into the range between 1/100 and 100. However, in the case of a very rigid girder (R<1/100) or very rigid support conditions (R>100), the fundamental natural frequency of a bridge becomes insensitive to the change in support stiffness.

Our previous studies[27] have shown that measuring the change in fundamental natural frequency provides an effective way for damage detection in the support areas of a bridge (e.g. degradation of bearing stiffness) but has limited capability in detecting corrosion and decrease in the materials properties of a bridge girder which usually do not significantly affect the overall structural integrity of a bridge. In addition, the present study shows that the developed SDOF model can only effectively detect the variation in bridge bearing stiffness when the ratio of the bearing stiffness to the girder stiffness (R) falls in the range between 1/100 to 100 which could lead to a detectable change in natural frequency.

Figure 9 shows the role of bridge bearing stiffness in fundamental natural frequencies of the M-80 and PoM bridges, respectively. The results also show that the effectiveness of developed SDOF is bridge dependent. For example, 40% decrease in bearing stiffness results in around 8% decrease in fundamental natural frequency of the M-80 Bridge but only 2% decrease in that of PoM Bridge. (The R-value for M-80 Bridge was 1.2 and PoM Bridge was 8.5).

5 Conclusions

The natural frequency of a bridge is one of the critical parameters which can be used to assess the structural health condition of the bridge. In this study, a bridge bearing monitoring method involving an analytical SDOF model and IBIS-FS was developed. The following are some major conclusions:

- The developed model can capture the dynamic characteristics of a bridge and estimate the mechanical stiffness of bridge bearing.
- The proposed model was validated by bridge field testing results using IBIS-FS in conjunction with FE analysis.

- The effectiveness of the model for detecting the deterioration of bearing stiffness is much dependent on the ratio between bridge bearing stiffness and girder stiffness (R).
- The developed model can only effectively predict the change in fundamental natural frequency due to the deterioration of bearing when R falls into the range between 1/100 and 100. However, in the case of very rigid girder (R<1/100) or very rigid support conditions (R>100), the fundamental natural frequency of a bridge becomes insensitive to the change in support stiffness.

6 Acknowledgments

The authors wish to thank the Australian Research Council (ARC IH150100006), Higher Education Commission Pakistan (HRDI – faculty development of UESTPs-UETs phase-1) and The University of Melbourne for their support. Also, the authors are grateful to VicRoads, Australia, and Port of Melbourne authorities, Australia.

References

1. Zhou R, Ge Y, Liu S, Yang Y, Du Y, Zhang L. Nonlinear flutter control of a long-span closed-box girder bridge with vertical stabilizers subjected to various turbulence flows. Thin-Walled Structures (Accepted on 11-June-2019) 2019.
2. Zhou R, Ge Y, Yang Y, Du Y, Liu S, Zhang L. Nonlinear behaviors of the flutter occurrences for a twin-box girder bridge with passive countermeasures. Journal of Sound and Vibration 2019;447(12):221-35.
3. Zhou R, Yang Y, Ge Y, Zhang L. Comprehensive evaluation of aerodynamic performance of twin-box girder bridges with vertical stabilizers. Journal of Wind Engineering and Industrial Aerodynamics 2018;175(317-327).
4. Zhou R, Ge Y, Yang Y, Du Y, Zhang L. Wind-induced nonlinear behaviors of twin-box girder bridges with various aerodynamic shapes. Nonlinear Dynamics 2018.
5. Yang Y, Zhou R, Ge Y, Zhang L. Flutter characteristics of thin plate sections for aerodynamic bridges. Journal of Bridge Engineering (ASCE) 2018;23(1):04017121-1-13.
6. Yang Y, Zhou R, Ge Y, Du Y, Zhang L. Sensitivity analysis of geometrical parameters on the aerodynamic performance of closed-box girder bridges. Sensors 2018;18(7):2053.
7. Zhou R, Yang Y, Zhang L, Ge Y. Interference effect on stationary aerodynamic performance between parallel bridges. International Journal of Structural Stability and Dynamics 2016;16(10):1750017-1-23.
8. Yang Y, Zhou R, Ge Y, Zhang L. Flutter characteristics of twin-box girder bridges with vertical central stabilizers. Engineering Structures 2017;133:33–48.
9. Yang Y, Zhou R, Ge Y, Zhang L. Experimental studies on VIV performance and countermeasures for twin-box girder bridges with various slot width ratios. Journal of Fluids and Structures 2016;66:476-89.
10. Wickramasinghe WR, Thambiratnam DP, Chan TH, Nguyen T. Vibration characteristics and damage detection in a suspension bridge. Journal of Sound and Vibration 2016;375:254-74.
11. Zhang L, Mendis P, Hon WC, Fragomeni S, Lam N, Song Y. Effects of cyclic loading on the long-term deflection of prestressed concrete beams. Computers and Concrete 2013;12(4):377-92.
12. Koh CG, Ang KK, Zhang L. Effects of repeated loading on creep deflection of reinforced concrete beams. Engineering Structures 1997;19(1):2-18.
13. Lai J, Zhang L, Duffield C, Aye L. Reliability Analysis in Risk Management Framework: Development and Application in Infrastructure Project. IAENG International Journal of Applied Mathematics 2013;43(4):242-9.
14. Kafle B, Zhang L, Mendis P, Herath N, Maizuar M, Duffield C, et al. Monitoring the dynamic behaviour of the Merlynston Creek bridge using interferometric radar sensors and finite element modelling. International Journal of Applied Mechanics 2017;9(1):1750003-1-20.
15. Raja BNK, Miramini S, Duffield C, Sofi M, Mendis P, Zhang L. The influence of ambient environmental conditions in detecting bridge concrete deck delamination using infrared thermography (IRT). Structural Control and Health Monitoring 2020;27(4):e2506.

16. Aria M, Akbari R. Inspection, condition evaluation and replacement of elastomeric bearings in road bridges. Structure and Infrastructure Engineering 2013;9(9):918-34.
17. Nguyen HH, Tassoulas JL. Directional effects of shear combined with compression on bridge elastomeric bearings. Journal of Bridge Engineering 2009;15(1):73-80.
18. Kim S-H, Mha H-S, Lee S-WJEs. Effects of bearing damage upon seismic behaviors of a multi-span girder bridge. 2006;28(7):1071-80.
19. Park Y-S, Kim S, Kim N, Lee J-J. Evaluation of bridge support condition using bridge responses. Structural Health Monitoring 2019;18(3):767-77.
20. Roeder CW, Stanton JF, Taylor AW, Performance of elastomeric bearings. 298. 1987.
21. Stanton JF, Roeder CW. Elastomeric bearings design, construction, and materials. NCHRP report 1982;(248).
22. Dicleli M, Bruneau M. An energy approach to sliding of single- span simply supported slab- on- girder steel highway bridges with damaged bearings. Earthquake engineering & structural dynamics 1995;24(3):395-409.
23. Watanabe E, Sugiura K, Nagata K, Kitane Y. Performances and damages to steel structures during the 1995 Hyogoken-Nanbu earthquake. Engineering Structures 1998;20(4-6):282-90.
24. Das S, Saha P, Patro S. Vibration-based damage detection techniques used for health monitoring of structures: a review. Journal of Civil Structural Health Monitoring 2016;6(3):477-507.
25. Maizuar M, Lumantarna E, Sofi M, Oktavianus Y, ZHANG L, Duffield C, et al. Dynamic behaviour of Indonesian bridges using interferometric radar technology. Electronic Journal of Structural Engineering 2018;18(1):23-9.
26. Zhang L, Maizuar M, Mendis P, Duffield C, Thompson R. Monitoring the dynamic behaviour of concrete bridges using non-contact sensors (IBIS-S). Applied Mechanics and Materials 2016;846:225-30.
27. Maizuar M, Zhang LH, Miramini S, Mendis P, Thompson RG. Detecting structural damage to bridge girders using radar interferometry and computational modelling. Struct Control Hlth 2017;24(10):e1985.
28. Yan Y, Cheng L, Wu Z, Yam L. Development in vibration-based structural damage detection technique. Mechanical systems and signal processing 2007;21(5):2198-211.
29. Kawiecki G. Modal damping measurement for damage detection. Smart Materials and Structures 2001;10(3):466.
30. Abdo M-B, Hori M. A numerical study of structural damage detection using changes in the rotation of mode shapes. Journal of Sound and vibration 2002;251(2):227-39.
31. Shi Z, Law S, Zhang LM. Structural damage detection from modal strain energy change. Journal of engineering mechanics 2000;126(12):1216-23.
32. Yam L, Yan Y, Jiang J. Vibration-based damage detection for composite structures using wavelet transform and neural network identification. Composite Structures 2003;60(4):403-12.
33. Yazdani N, Eddy S, Cai CS. Effect of bearing pads on precast prestressed concrete bridges. Journal of Bridge Engineering 2000;5(3):224-32.
34. Wolf JA, The influence of mounting stiffness on frequencies measured in a vibration test. SAE Technical Paper, 1984.
35. Lee PK, Ho D, Chung H-W. Static and dynamic tests of concrete bridge. Journal of Structural Engineering 1987;113(1):61-73.
36. Kang K-H, Kim K-J. Modal proporties of beams and plates on resilient supports with rotational and translational complex stiffness. Journal of sound and vibration 1996;190(2):207-20.
37. Dai W, Moroni MO, Roesset J, Sarrazin M. Effect of isolation pads and their stiffness on the dynamic characteristics of bridges. Engineering structures 2006;28(9):1298-306.
38. Memory T, Thambiratnam D, Brameld G. Free vibration analysis of bridges. Engineering Structures 1995;17(10):705-13.
39. Memory T. On the dynamic behaviour of highway bridges. Master of Engineering Thesis, Queensland University of Technology, Australia 1992.
40. Fayyadh MM, Razak HAJC, Materials B. Condition assessment of elastic bearing supports using vibration data. 2012;30:616-28.
41. MacBain J, Genin J. Effect of support flexibility on the fundamental frequency of vibrating beams. Journal of the Franklin Institute 1973;296(4):259-73.
42. Rao CK, Mirza S. A note on vibrations of generally restrained beams. Journal of Sound and Vibration 1989;130(3):453-65.
43. Carne TG, Dohrmann CR. Support conditions, their effect on measured modal parameters. In Proceedings of the PROCEEDINGS-SPIE THE INTERNATIONAL SOCIETY FOR OPTICAL ENGINEERING, 1998. SPIE INTERNATIONAL SOCIETY FOR OPTICAL;477-83.
44. Cebon DJVsd. Vehicle-generated road damage: a review. 1989;18(1-3):107-50.

45. Green MF, Cebon D, Cole DJJJoSE. Effects of vehicle suspension design on dynamics of highway bridges. 1995;121(2):272-82.
46. Hongge LJTE, Defence TfN. A Comparative Study of the Dynamic Behavior of Viaducts Respectively with Single-Column Cantilever Bent Cap and with Double-Column Piers. 2012;1.
47. Barth KE, Wu HJES. Development of improved natural frequency equations for continuous span steel I-girder bridges. 2007;29(12):3432-42.
48. McLean DI, Marsh ML, Dynamic impact factors for bridges. Transportation Research Board, 1998.
49. Quality OMoT, Division S, Ontario highway bridge design code. Government of Ontario, 1991.
50. Bartos MJ. Ontario writes new bridge code. Civil Engineering—ASCE 1979;49(3):56-61.
51. Comsol A. Comsol Multiphysics: Structural Mechanics Module. User's Guide 2018.
52. Yang Y, Lam N, Zhang L. Estimation of response of plate structure subject to low veloctiy impact by a solid object. International Journal of Structural Stability and Dynamics 2012;12(06):1250053.
53. Mothe RN. Partial continuity in prestressed concrete girder bridges with jointless decks. 2006.
54. Shi Y, Chan S, Wong Y. Modeling for moment-rotation characteristics for end-plate connections. Journal of Structural Engineering 1996;122(11):1300-6.
55. Duarte Da Costa J, Braun MV, Obiala R, Odenbreit C. Design of single-span beams for SLS and ULS using semi-continuous beam-to-column joints. Part 2: Composite beams with variable bending stiffness and joints according to EN 1993-1-8. Steel Construction 2017;10(2).
56. Couchman GH, Design of semi-continuous braced frames. Steel Construction Institute Ascot, 1997.

List of Tables

Table 1. Material properties of selected bridges

Parameter	Unit	Girder Concrete	Slab Concrete	Rebars	Tendon
Bridge Description		PoM Bridge / M-80 Bridge			
Mass density	kg/m^3	2550/2400	2600/2400	7850	7850
Poisson's ratio	-	0.2	0.2	0.3	0.33
Youngs Modulus	*MPa*	35,000/34800	35,000/32800	200,000	200,000
Springs/ bearing pad stiffness	*kN/m*		690,000/168000		

Table 2. Generalised stiffness of beam/girder

End restraints	Continuous/fully restrained	Semi-continuous / partially restrained
Simply supported	$\alpha = \pi$	-
Fixed-Fixed	$\alpha = \pi + \pi/2$	$\alpha = \pi + (\pi/2)\,.\,\kappa$
Fixed-Pin	$\alpha = \pi + \pi/4$	$\alpha = \pi + (\pi/4)\,.\,\kappa$

*κ = stiffness coefficient of bridge that incorporates the effects of semi-rigid restraints conditions on the elastic stiffness of the bridge girder ***(k_b)*** (Figure 5b).

Table 3. FE model results comparison with IBIS-FS test results

	Natural frequency (Hz)			
Method	**Port Melbourne Bridge, Melbourne**		**Merlynston Creek bridge, M-80**	
	1st mode	***2nd mode***	***1st mode***	***2nd mode***
Field test (IBIS-FS)	4.1	6.08	9.4	15.5
FE prediction	3.88	5.97	9.55	15.75

Table 4. Elastic stiffness calculation for M-80 and PoM bridges with semi-continuous girders

Bridge	Slab end-restrain	Structural member	E^* (N/m^2)	I^* (slab) (m^4)	I^* (total) (m^4)	L (m)	$n = \frac{(EI)_c}{\frac{(EI)_b}{L_b}}$	κ	α	k_b (kN/m m)
M-80	Fixed-Fixed	Slab/Girder	32.8×10^9/ 34.8×10^9	0.0011	0.0579	13.5	0.26	0.35	1.175π	140.8
PoM	Fixed-Pin	Slab/Girder	35.0×10^9/ 35.0×10^9	0.0012	0.351	30.0	0.104	0.24	$1.06\,\pi$	61.25

*the given properties correspond to single girder area only

Table 4. SDOF model results comparison with IBIS-s test results

Method	Port Melbourne Bridge, Melbourne		Merlynston Creek bridge, M-80	
	Natural frequency (Hz)	***% difference***	***Natural frequency (Hz***	***% difference***
Field test (IBIS-FS)	4.1	5.3%	9.4	0.2%
SDOF model	3.87		9.42	

FIGURES

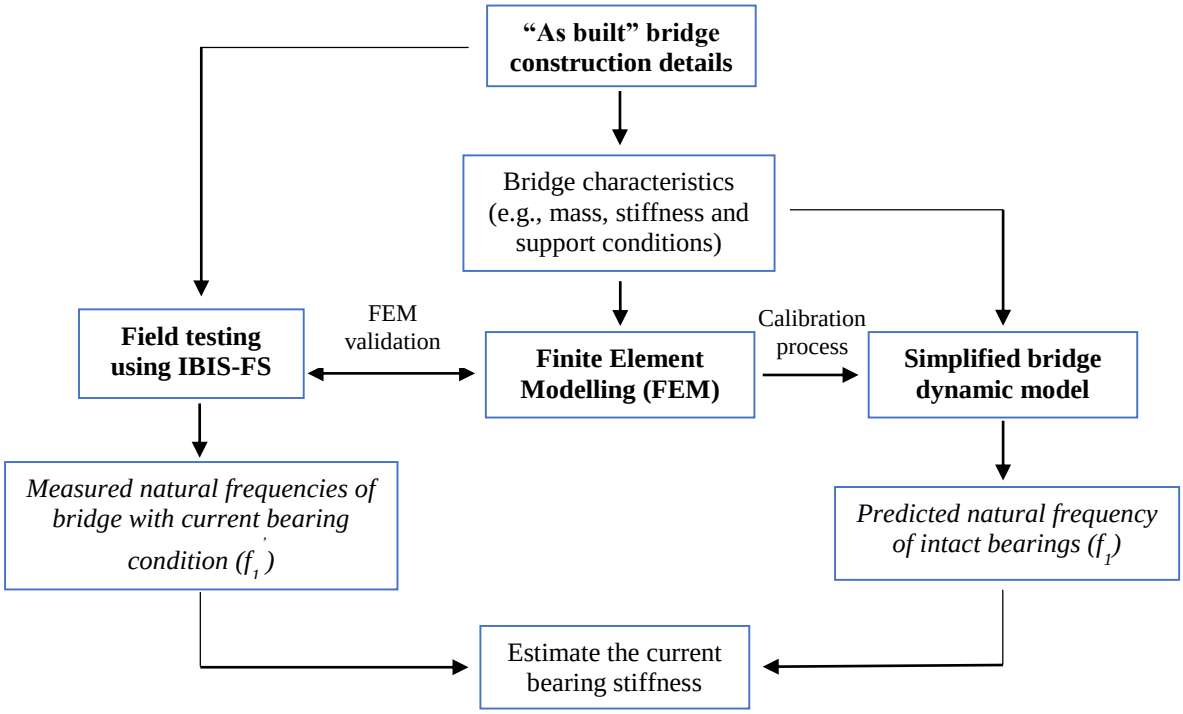

Fig. 1. A schematic framework to estimate the current bridge bearing stiffness using simplified bridge dynamic model in conjunction with field testing using interferometric radar (IBIS-FS)

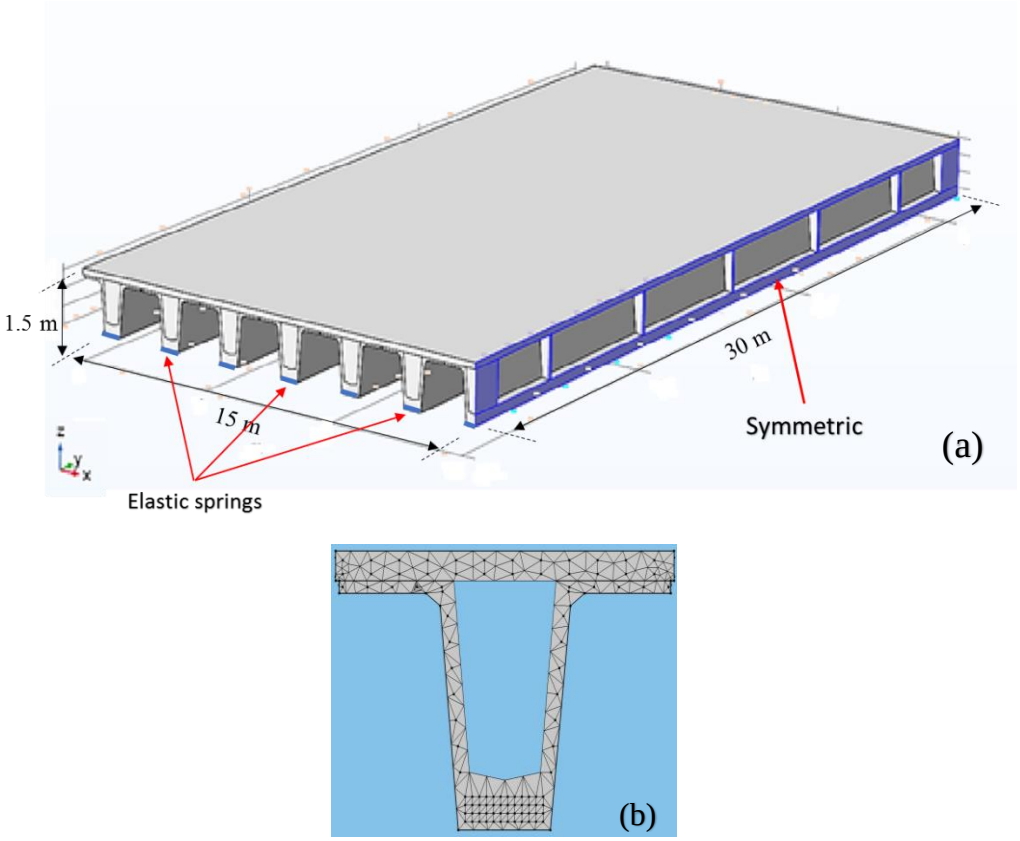

Fig. 2. (a) FE model of Port Melbourne bridge (b) FE model of super T-girder for sensitivity analysis; typical cross-section.

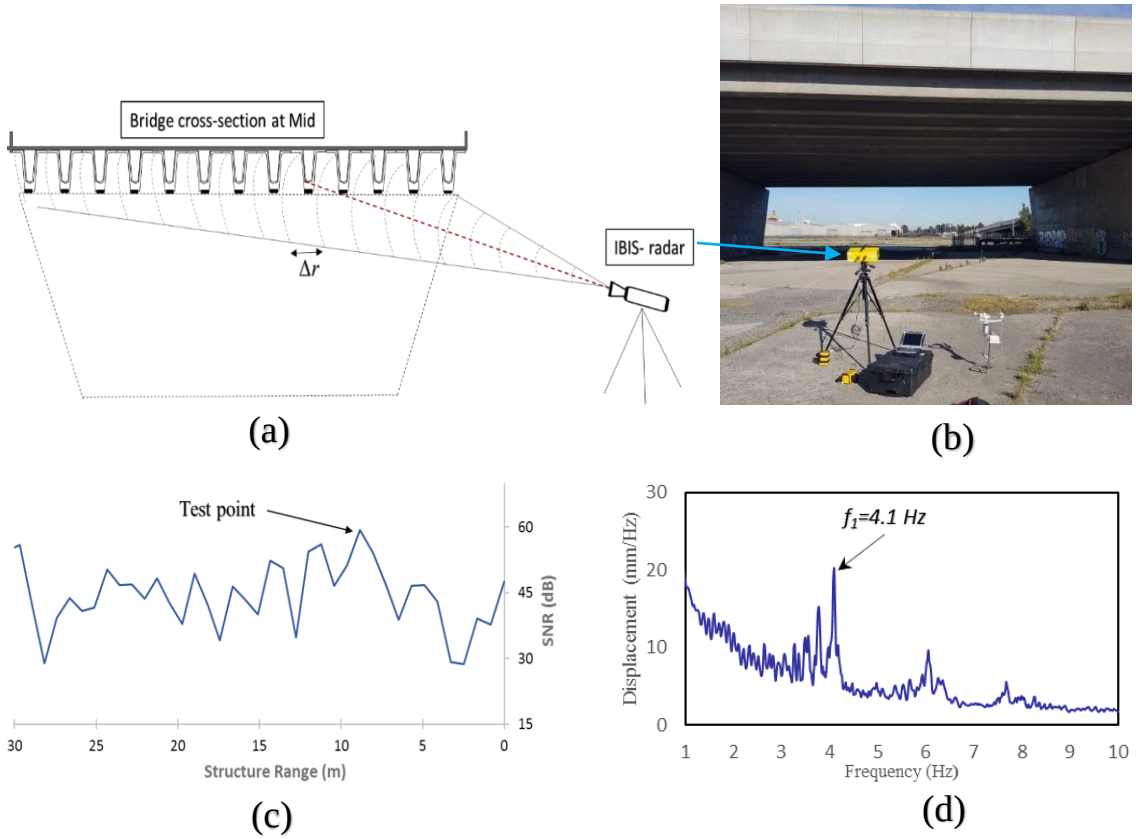

Fig. 3. Field testing of PoM bridge; (a) IBIS-s configuration, (b) Field testing setup, (c) Radar echo intensities from different range bins as a function of range profile of bridge cross-section, and (d) Measured natural frequency of bridge generated from experimental dataset

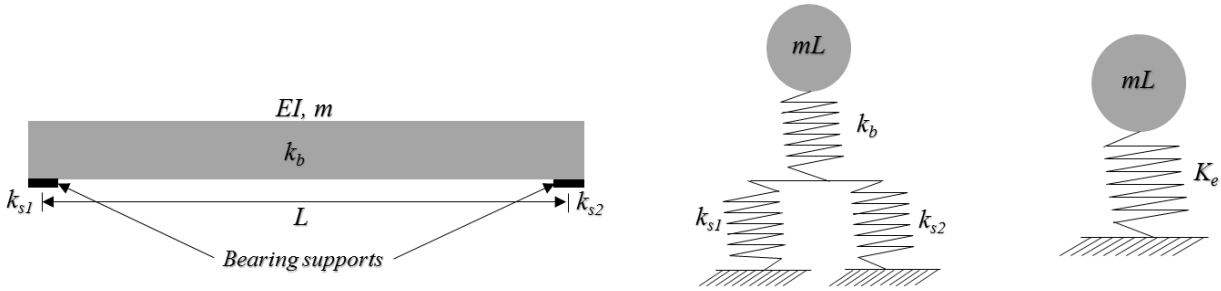

Fig. 4. Simplified bridge dynamic model using single degree of freedom (SDOF) approach (k_s = stiffness of bearings, k_b= stiffness of girders, K_e=effective stiffness of overall system)

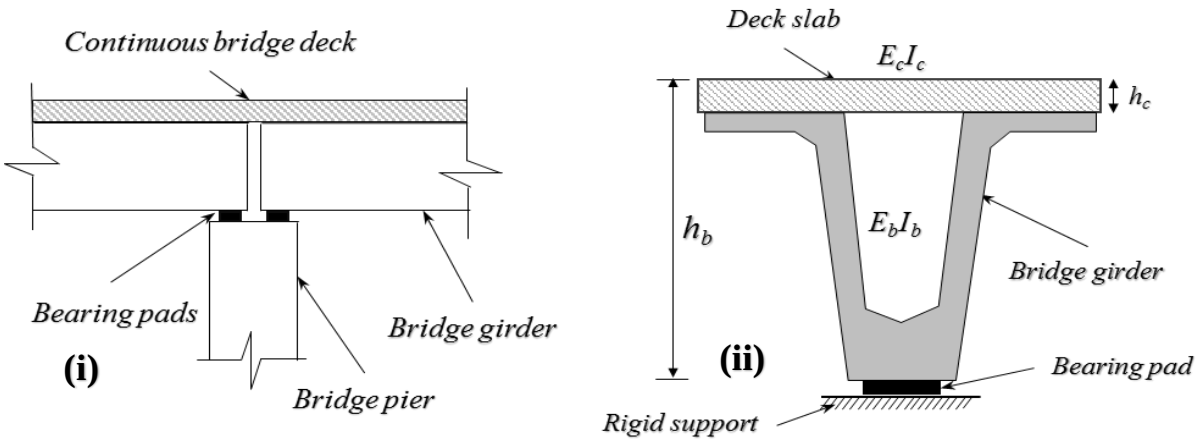

Fig. 5a. Support conditions of bridge girder, (i) elevation (ii) cross-section

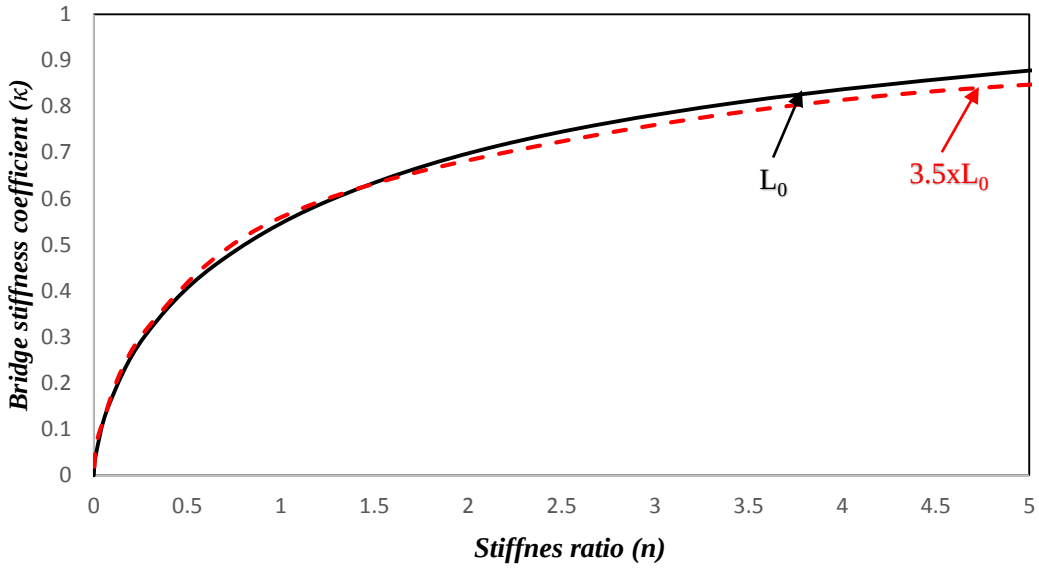

Fig. 5b. Bridge stiffness coefficient (κ) as a function of ratio of flexural rigidity of continuous slab deck and bending stiffness of the girder beam n= (E_c I_c) / (E_bI_b / L_b); (L_0 = 10m)

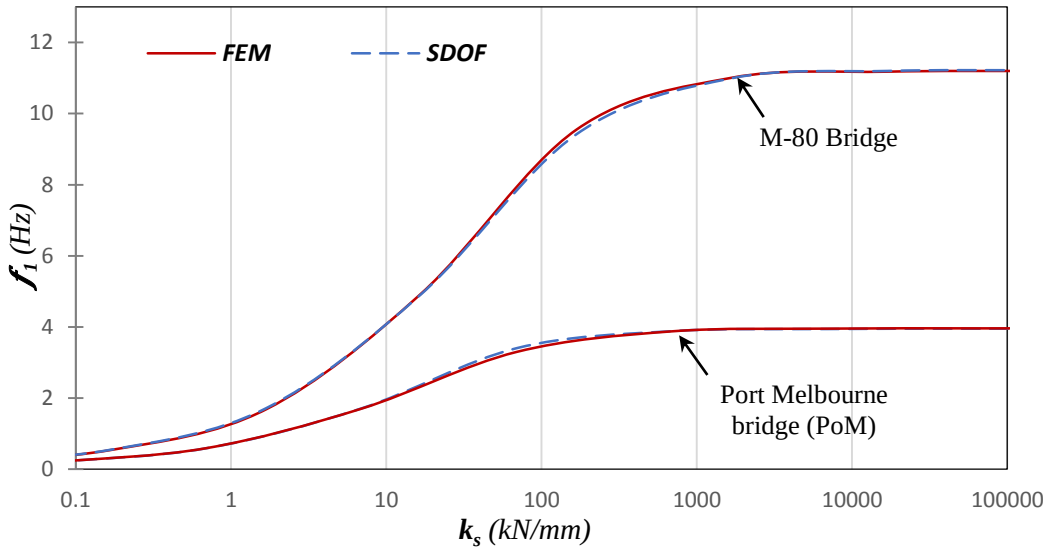

Fig. 6. Effect of bearing stiffness variation on fundamental frequency of the bridge

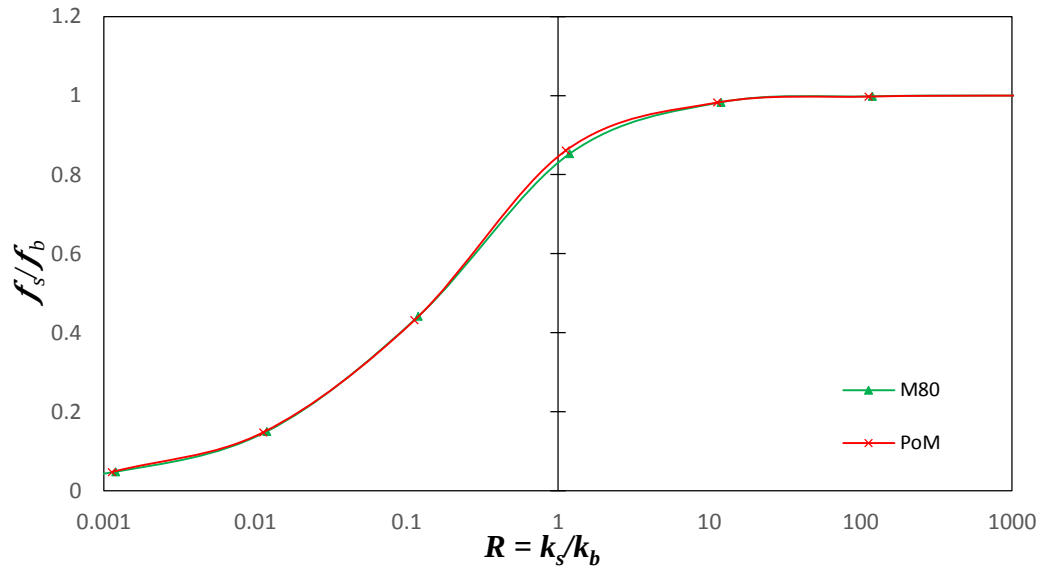

Fig. 7. Effect of stiffness ratios (R) on fundamental frequency of system (k_s = stiffness of spring, f_s = natural frequency of system with flexible supports, k_b= stiffness of girder, f_b= natural frequency of system with rigid supports)

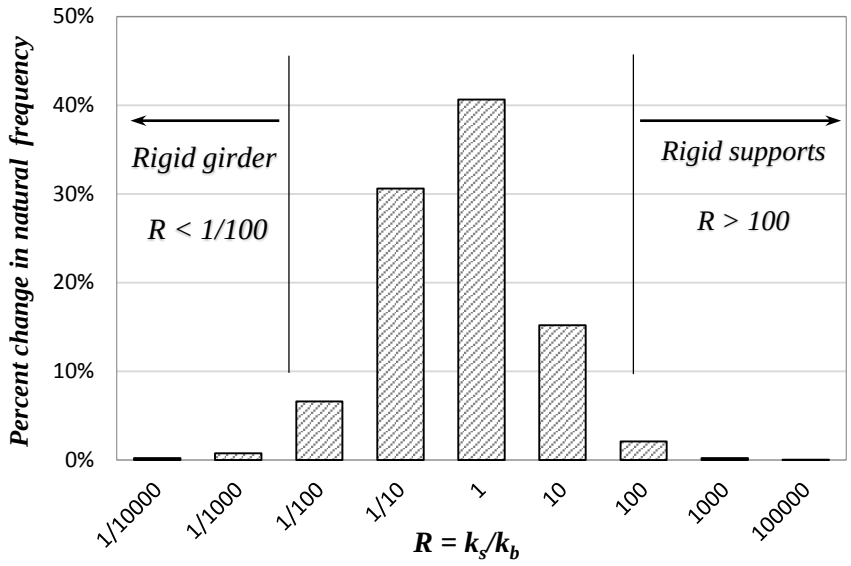

Fig. 8. Percent change in frequency with the change in stiffness ratio, R (k_s = stiffness of spring, k_b= stiffness of girder)

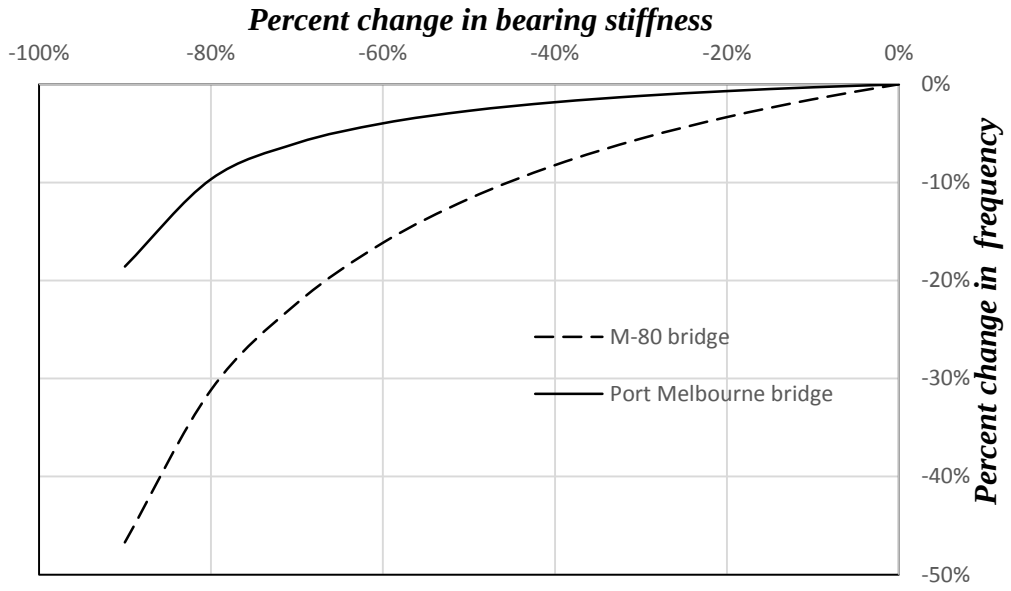

Fig. 9. Change in natural frequency of M-80 and PoM bridges with change in bearing stiffness